Proceedings of 26th International Scientific Conference. Transport Means 2022.

Predicting Dust Pollution in the Passenger Compartment

M. Biliaiev[1], T. Rusakova[2], V. Biliaieva[3], P. Mashykhina[4], K. Rusakova[5]

[1]*Ukrainian State University of Science and Technology, Lazaryan, 2, 49010, Dnipro, Ukraine,*
E-mail: biliaiev.m@gmail.com
[2]*Oles Honchar Dnipro National University, Haharin av. 72, 49010, Dnipro, Ukraine, E-mail: rusakovati1977@gmail.com*
[3]*Oles Honchar Dnipro National University, Haharin av. 72, 49010, Dnipro, Ukraine, E-mail: biliaiev.m@gmail.com*
[4]*Ukrainian State University of Science and Technology, Lazaryan, 2, 49010, Dnipro, Ukraine,*
E-mail: gidro_eko@ukr.net
[5]*Oles Honchar Dnipro National University, Haharin av. 72, 49010, Dnipro, Ukraine, E-mail: rusakova9925@gmail.com*

Abstract

Fine dust particles, which are present in the air in large quantities, are dangerous to human health. They enter the body through the lungs, but move to almost all organs, causing a number of respiratory diseases, pneumonia and are carriers of the coronavirus. This research proposes a method for numerically calculating the process of dust pollution of the passenger compartment when fine dust enters the cabin through the ventilation system. To calculate the concentration field of dust in the cabin, the equation of convective-diffusion dust dispersion is used, which takes into account the intensity of dust entering the passenger compartment, the unevenness of the air flow velocity field in the passenger compartment, diffusion, and additional dust emission from the floor surface. To calculate the velocity field of the air flow in the car interior, a potential flow model is used, the modeling equation is the Laplace equation for the velocity potential. For the numerical integration of the convective-diffusion dispersion equation of fine dust in the cabin, implicit finite-difference splitting schemes are used. For the numerical solution of the equation for the aerodynamic velocity potential, the alternating-triangular method of A. Samarsky is used. The computer code has been developed that implements the method of numerical calculation. The results of computational experiments to assess the level of dust pollution in the passenger compartment are presented.
KEY WORDS: *auto transport, air pollution, canyon, velocity field, pollution concentration level, difference methods*

1. Introduction

Air pollution is one of the most studied environmental issues worldwide as it poses a constant threat to human health and quality of life. Dust particles are one of the main threats to human health, especially in large urbanized cities, where the level of air pollution is constantly increasing. This impurity particles consist of a complex mixture of chemical and biological components [1-2]. The aerodynamic parameters of these particles are different, they are determined by the source of pollution, particle size, meteorological parameters of the air [3]. These particles are classified as large (2.5–10 μm), small (0.1–2.5 μm), and ultrafine (< 0.1 μm) [4]. The degree of toxicity increases with decreasing of the size of particles. These particles can enter the lungs and enter the vital organs due to their small size [5, 6], causing serious consequences for human health: cardiovascular and respiratory diseases [7], asthma attacks and bronchitis, allergic diseases, diabetes the second type [8].

The motor transport is one of the sources of fine particles. The type of ventilation determines the level of concentration of harmful substances in the passenger compartment, as well as the quality of the inlet and cabin filters [9]. The small size of a passenger compartment results in passengers being exposed to high concentrations of fine particles that may not be captured by car filters. This has an impact on the general state of health of a person. A number of studies are devoted to the issues of measurement of gaseous impurities in the passenger compartment [10, 11]. However, the distribution of fine dust in the car interior is poorly understood. The urgency of solving this problem lies in the fact that when recommending the use of filters for a particular cabin, it is necessary to carry out preliminary estimates of the spread of dust concentration throughout the passenger compartment. The devices for measuring impurity concentration fix the concentration value locally at a specific point, and not in the entire area of the car passenger compartment, which is a more significant result of the study.

In this paper, we consider the problem of calculating the dust concentration field inside the passenger compartment when fine dust enters the cabin through the ventilation system or due to dust emission from the floor surface. The solution of this problem is based on the developed method for numerical calculation of the dust concentration in the passenger compartment. This method is based on the equation of convective-diffusion dust scattering, which is solved by a finite difference method.

2. Statement of the Problem and Its Solution

2.1. Mathematical Model

The interior of the Isuzu Mu-X car is considered in the form of ABCDEFGHKL in the *Oxy* plane coordinate system. The cutting plane is drawn at a distance of 0.48 m from the central section of the car. Typical geometric dimensions of the area: height – 180 cm, length - 480 cm, distance from the back of the front seat to the steering wheel – 85 cm, distance between the seat backs – 90 cm (Fig. 1).

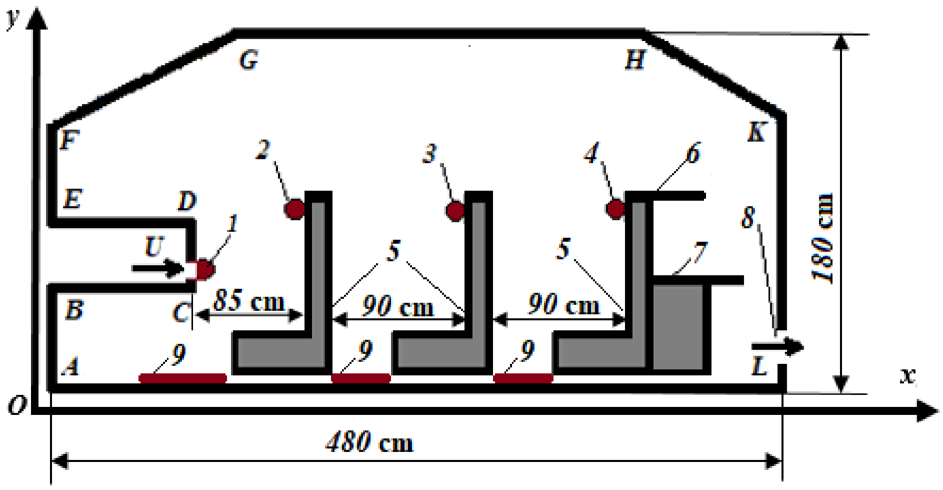

Fig. 1 Scheme of the calculation area of passenger compartment: *1* – dust source; *2,3,4* – passenger head; *5* – seats; *6* – shelf behind the back seat; *7* – obstacles in the car trunk, *8* – exhaust opening, *U* – air speed in supply ventilation; *9* – floor surface (source of dust)

The task is to study the dust concentration field in the passenger compartment. Fine dust enters through the vent (position 1, Fig. 1) and from the floor surface (position 9, Fig. 1). A two-dimensional mass transfer equation is used to calculate the dust concentration field, taking into account the interaction of various dust sources, diffusion, and the uneven air velocity field in the passenger compartment. The modeling equations have the form (1) [13]:

$$\frac{\partial C}{\partial t}+\frac{\partial uC}{\partial x}+\frac{\partial vC}{\partial y}=\frac{\partial}{\partial x}\left(\mu_x\frac{\partial C}{\partial x}\right)+\frac{\partial}{\partial y}\left(\mu_y\frac{\partial C}{\partial y}\right)+\sum_{i=1}^{N}Q_i(t)\delta\left(x-x_i,y-y_i\right). \quad (1)$$

The designations of the physical parameters in these equations are as follows:

$C(x,y,t)$ – dust particle concentration, [mg/м^3]; $u(x,y)$, $v(x,y)$ – air velocity components in the passenger compartment, [m/s]; μ_x, μ_y – diffusion coefficients, [m^2/s], $\mu_x=0.1\cdot u(x,y)$, $\mu_y=0.1\cdot v(x,y)$; t – time, [s]; $Q_i(t)$ – dust emission intensity, [mg/(s·m^3)]; x_i, y_i – coordinates of dust emission sources, [m]; $\delta(x-x_i,y-y_i)$ – Dirac delta function. The *Oy* axis is directed vertically upwards, the *Ox* axis is directed along the passenger compartment (Fig. 1). The delta function is equal to zero everywhere, except for the cells in which the i-th emission source is located.

To solve Eq. (1), the following boundary and initial conditions are set (Fig. 1):

– at the boundary of the *CD* airflow entry into the passenger compartment, the dust concentration $C=C_{entrance}$ – background dust concentration at time $t=0$, in the absence of data, the concentration value $C_{entrance}$ is assumed to be zero, $C_{entrance}=0$;

– on all solid walls (car body, seats), depending on the direction of the normal, the non-penetration condition must be satisfied, which requires that the change in concentration along the normal to the surface be equal to zero.

– at the boundary of the exit of the air flow *KL* from the passenger compartment, the diffusion process is not taken into account.

– at the initial moment of time, it is assumed that the dust concentration in the cabin is equal to zero. If necessary, you can set any other dust value, for example, determined by experimental measurements.

When the air environment moves in the car interior, an uneven field of air flow velocity is formed. This greatly complicates the solution of the problem of determining the dust concentration field in the cabin. Inside the cabin there are seats that represent the movement of air, changing its direction. Besides, the position of the supply and exhaust openings also determine the aerodynamics of the air flows in the cabin. To solve the transfer equation (1), it is necessary to calculate the components of the air flow velocity vector *u*, *v* in the passenger compartment. The determination of the components of the air velocity vector in the passenger compartment is based on the potential flow model [12]. It is necessary to integrate the Laplace Eq. (2) for the velocity potential *P*:

$$\frac{\partial^2 P}{\partial x^2}+\frac{\partial^2 P}{\partial y^2}=0\,. \qquad (2)$$

To solve equation (2), the following boundary and initial conditions are set (Fig. 1):

– at the border of the *CD* inlet (position 1 Fig. 1) of the air flow into the passenger compartment at a speed U the boundary condition is set $\frac{\partial P}{\partial x}=U$;

– at the boundary of the outlet KL of the air flow from the computational domain, where the exhaust hole is located (position 8 in Fig. 1), the boundary condition is set for the velocity potential $P=P_0+const$, where P_0 – some numeric constant;

– on solid impenetrable boundaries (cabin walls, seat surfaces), including the lower and upper boundaries of the area, a non-penetration condition is set $\frac{\partial P}{\partial n}=0$, where $\vec{n}$ – the unit outward normal vector at the given boundary.

The components of the airflow velocity vector are calculated based on (3) [12]:

$$u=\frac{\partial P}{\partial x}\,,\ v=\frac{\partial P}{\partial y}\,. \qquad (3)$$

2.2. Numerical Model

Numerical integration of modeling equations (1) – (3) is performed on a rectangular grid.

For numerical integration of Eq. (1), it is split into three Eqs. (4) – (6) [11].

$$\frac{\partial C}{\partial t}+\frac{\partial uC}{\partial x}=\frac{\partial}{\partial x}\left(\mu_x\frac{\partial C}{\partial x}\right)\ ; \qquad (4)$$

$$\frac{\partial C}{\partial t}+\frac{\partial vC}{\partial y}=\frac{\partial}{\partial y}\left(\mu_y\frac{\partial C}{\partial y}\right)\ ; \qquad (5)$$

$$\frac{\partial C}{\partial t}=\sum_{i=1}^{N}Q_i(t)\cdot\delta(x-x_i,y-y_i)\ . \qquad (6)$$

For the numerical integration of Eq. (4), a two-step splitting scheme (7) – (8) is used:

– in the first step:

$$C_{i,j}^{n+\frac{1}{2}}=C_{i,j}^{n}-\Delta t\,\frac{u_{i+1,j}^{+}C_{i,j}^{n+\frac{1}{2}}-u_{i,j}^{+}C_{i-1,j}^{n+\frac{1}{2}}}{\Delta x}+\Delta t\,\mu_x\,\frac{-C_{i,j}^{n+\frac{1}{2}}+C_{i-1,j}^{n+\frac{1}{2}}}{2\Delta x^2}+\Delta t\,\mu_x\,\frac{-C_{i,j}^{n}+C_{i+1,j}^{n}}{2\Delta x^2}\ ; \qquad (7)$$

– in the second step:

$$C_{i,j}^{n+1}=C_{i,j}^{n+\frac{1}{2}}-\Delta t\,\frac{u_{i+1,j}^{-}C_{i+1,j}^{n+1}-u_{i,j}^{-}C_{i,j}^{n+1}}{\Delta x}+\Delta t\,\mu_x\,\frac{-C_{i,j}^{n+\frac{1}{2}}+C_{i-1,j}^{n+\frac{1}{2}}}{2\Delta x^2}+\Delta t\,\mu_x\,\frac{-C_{i,j}^{n+1}+C_{i+1,j}^{n+1}}{2\Delta x^2}\ , \qquad (8)$$

where $u^{+}=\frac{u+|u|}{2}$, $u^{-}=\frac{u-|u|}{2}$.

For the numerical integration of equation (5), a two-step splitting scheme (9) – (10) is used:

– in the first step:

$$C_{i,j}^{n+\frac{1}{2}}=C_{i,j}^{n}-\Delta t\,\frac{v_{i,j+1}^{+}C_{i,j}^{n+\frac{1}{2}}-v_{i,j}^{+}C_{i,j-1}^{n+\frac{1}{2}}}{\Delta y}+\Delta t\,\mu_y\,\frac{-C_{i,j}^{n+\frac{1}{2}}+C_{i,j-1}^{n+\frac{1}{2}}}{2\Delta y^2}+\Delta t\,\mu_y\,\frac{-C_{i,j}^{n}+C_{i,j+1}^{n}}{2\Delta y^2}\ ; \qquad (9)$$

– in the second step:

$$C_{i,j}^{n+1}=C_{i,j}^{n+\frac{1}{2}}-\Delta t\,\frac{v_{i,j+1}^{-}C_{i,j+1}^{n+1}-v_{i,j}^{-}C_{i,j}^{n+1}}{\Delta y}+\Delta t\,\mu_y\,\frac{-C_{i,j}^{n+\frac{1}{2}}+C_{i,j-1}^{n+\frac{1}{2}}}{2\Delta y^2}+\Delta t\,\mu_y\,\frac{-C_{i,j}^{n+1}+C_{i,j+1}^{n+1}}{2\Delta y^2}\ , \qquad (10)$$

where $v^{+} = \frac{v+|v|}{2}$, $v^{-} = \frac{v-|v|}{2}$.

For the numerical integration of Eq. (6), the Euler method is used [12].

Next, the Laplace Eq. (2) is reduced to an equation of an "evolutionary" form using the establishment of a solution in time [12]:

$$\frac{\partial P}{\partial \varsigma} = \frac{\partial^2 P}{\partial x^2} + \frac{\partial^2 P}{\partial y^2}, \tag{11}$$

where ς – fictitious time, when $\varsigma \to \infty$, the solution of Eq. (11) tends to the solution of the Laplace Eq. (2). The stationary Eq. (2) is the limiting case of the non-stationary Eq. (11).

To solve Eq. (11), the initial condition is set: $P = 0$ in the entire computational domain at $\varsigma = 0$.

Numerical integration is performed taking into account the difference approximation of derivatives on a rectangular grid $(x,\, y)_{i,j} = (i \cdot \Delta x,\, j \cdot \Delta y)$, $i, j \in Z$, time is uniformly discretized $\varsigma = n \cdot \Delta\varsigma$. The function $P(x, y, \varsigma)$ is expressed at any node by a discrete analog $P(x, y, \varsigma) = P(i \cdot \Delta x,\, j \cdot \Delta y,\, n \cdot \Delta\varsigma) = P^n_{i,j}$ [12].

Eq. (11) is geometrically split into two Eq. (12):

$$\frac{\partial P}{\partial \varsigma} = \frac{\partial^2 P}{\partial x^2}, \quad \frac{\partial P}{\partial \varsigma} = \frac{\partial^2 P}{\partial y^2}. \tag{12}$$

The use of an explicit difference scheme makes it possible to obtain the relations [12]:

$$\begin{cases} P^{n+1}_{i,j} = P^n_{i,j} + \Delta\varsigma \dfrac{P^n_{i+1,j} - P^n_{i,j}}{\Delta x^2} + \Delta\varsigma \dfrac{-P^n_{i,j} - P^n_{i-1,j}}{\Delta x^2}; \\ P^{n+1}_{i,j} = P^n_{i,j} + \Delta\varsigma \dfrac{P^n_{i,j+1} - P^n_{i,j}}{\Delta y^2} + \Delta\varsigma \dfrac{-P^n_{i,j} - P^n_{i,j-1}}{\Delta y^2}. \end{cases} \tag{13}$$

The calculation ends when the condition is met $\left|P^{n+1}_{i,j} - P^n_{i,j}\right| \le \varepsilon$, where ε – calculation accuracy, $\varepsilon = 10^{-3} \div 10^{-6}$, n – iteration number (number of time steps), when performing calculations, it was taken $\varepsilon = 0{,}0001$.

Based on the known values of the velocity potential, the local components of the air flow velocity on the sides of the difference cells are calculated [12]:

$$u_{i,j} = \frac{P_{i+1,j} - P_{i,j}}{\Delta x}, \quad v_{i,j} = \frac{P_{i,j+1} - P_{i,j-1}}{\Delta y}. \tag{14}$$

The software implementation "DUST-2" of the developed numerical calculation method was created in the FORTRAN programming language.

2.3. Results of Computational Experiments

The developed numerical method was applied to solve the problem of predicting dust pollution in the interior of an Isuzu Mu-X car, the computational area is schematically shown in Fig. 1.

Dust pollution enters the car interior through the ventilation opening located on the control panel (position 1, Fig. 1) $Q_{entrance}$ = 0.19 mg/s, since the fine dust in the incoming air is not completely retained by the filter. Additional sources of dust are located on the cabin floor in front of the first, second and third seats, in the area where the passengers' feet are located (position 9 Fig. 1). The dust emission intensity in front of the first seat is Q_i = 0.0052 mg/s, in front of the second and third seats Q_i = 0.0026 mg/s. Geometric dimensions of the computational domain: length – 4.8 m, height – 1.8 m; air flow rate – 0.55 м/с; the settling rate of fine dust entering the cabin was assumed to be 0 m/s. The concentration value is presented as a percentage of the maximum in the calculation area.

The Fig. 2 shows the dust concentration field when the dust came only from the ventilation opening (position 1, Fig. 2). The maximum dust concentration gradient is observed near the first seat, area A – 30-35%, near the respiratory organs of the first passenger (position 2, Fig. 2) does not exceed 5-10%, near the respiratory organs of the second and third passengers (position 3-4, Fig. 2) less than 5% of the maximum dust concentration C_{max} = 0.19 mg/m^3.

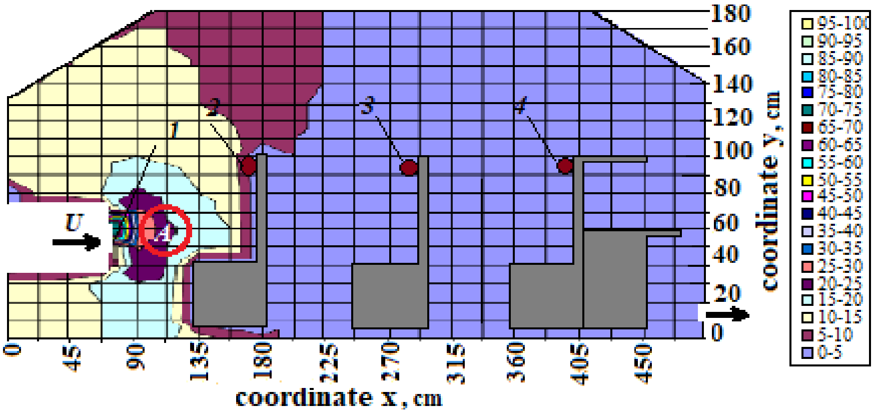

Fig. 2 The field of dust concentration in the passenger compartment, C_{max} = 0.19 mg/m^3

The Fig. 3 shows the dust concentration field when the dust came not only from the ventilation opening (position 1, Fig. 3), but also from the floor of the passenger compartment (position *D*, Fig. 3). The maximum dust concentration gradients are observed near each of the chairs, area A – 60-80%, area B – 40-60%, area A – 25-45%. Near the respiratory organs of the first passenger 30-35%, near the respiratory organs of the second passenger – 20-25%, near the respiratory organs of the third passenger less than 10-15% of the maximum dust concentration C_{max} = 0.38 mg/m^3.

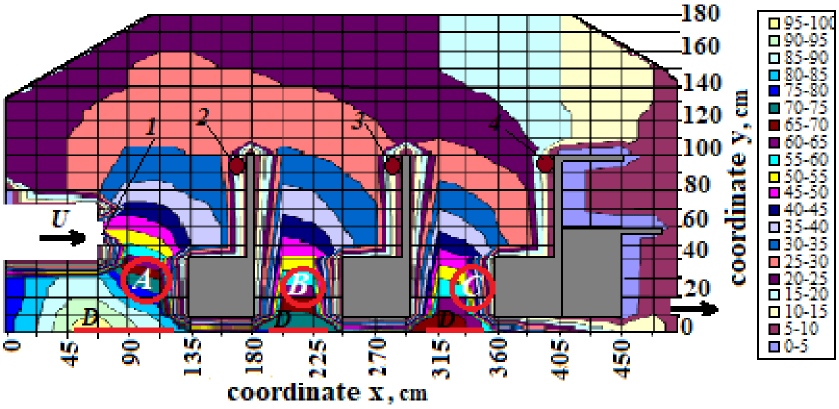

Fig. 3 The field of dust concentration in the passenger compartment, C_{max} = 0.38 mg/m^3

The analysis of the concentration field in Fig. 2 – Fig. 3 shows that a significant influence on the level of dust concentration in the car interior is exerted by the dust that is brought into the cabin by passengers with their shoes. Since the dust that enters through the inlet vent moves to the top of the cabin, where nothing prevents its movement, it is therefore quickly dissipated due to the action of exhaust ventilation. Dust coming from the floor of the cabin cannot move freely due to the seats, so the concentration of dust near the respiratory organs of passengers is much bigger.

The Fig. 4 shows the distribution of dust concentration at the height of the seats for both cases. For the first case, when the source of dust was only from the ventilation opening, at the level of the head of the first passenger C_1 = 0.021 mg/m^3, second C_2 = 0.0057 mg/m^3, third C_3 = 0.0019 mg/m^3 (Fig. 4 a). For the second case, when the source of dust was from the ventilation opening and the floor, at the level of the head of the first passenger C_1 = 0.11 mg/m^3, second C_2 = 0.097 mg/m^3, third C_3 = 0.076 mg/m^3 (Fig. 4 b).

The analysis of the dust concentration distribution at the level of the passengers' heads shows that when taking into account the source of dust emission from the floor, the concentration value near the head of the first passenger increases five times, near the head of the second passenger – 17 times, near the head of the third passenger – 40 times. This is explained by the fact that the chairs create a large obstacle to the movement of the polluted flow, which moves from below, from the floor of the passenger compartment upwards, but encounters an obstacle on its way, thereby being localized at the location of the dust source. The concentration of dust at the level of the head of all passengers varies slightly, it decreases from 8% – near the head of the second passenger to 30% – near the head of the third passenger, compared with the concentration near the head of the first passenger. Whereas in the first case, when only the source of dust from the ventilation opening was taken into account, the concentration value rapidly decreases from 70% near the head of the second passenger to 90% near the head of the third passenger, compared with the concentration near the head of the first passenger.

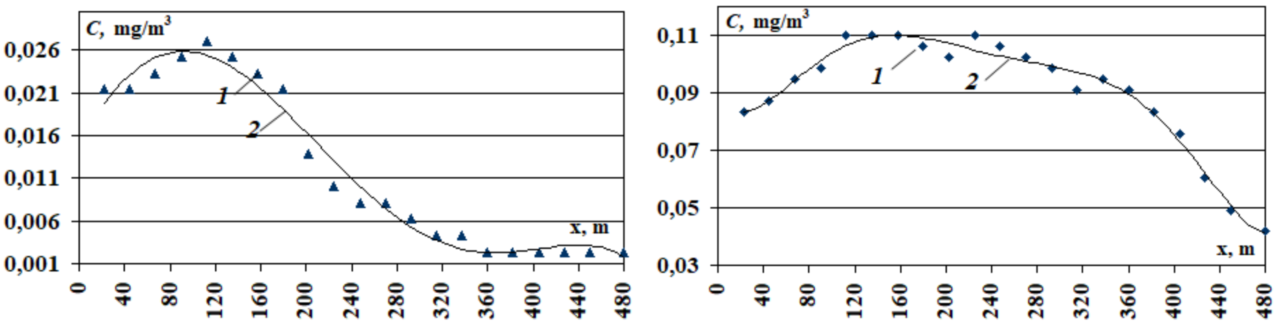

ab

Fig. 4 Graph of the distribution of dust concentration in the passenger compartment at the height of the seats: a – source of dust from the ventilation opening; b – source of dust from the ventilation opening and floor; *1* – numerical calculation; *2* – polynomial curve

In this study, based on the developed method of numerical calculation, an analysis was made of the influence of a different number of dust sources in the passenger compartment on the level of dust concentration. The possibilities of applying this method with respect to various options for the location of sources of dust of various intensity are shown. The need to use additional sources of ventilation inside the passenger compartment was proved.

3. Conclusions

A numerical method is proposed for calculating the dust concentration field in the passenger compartment, which allows taking into account: the geometry of the car, the height of the seats, their number, the different intensity of the dust source and their number. This method makes it possible to obtain the concentration value both locally and in the entire computational domain. Computational experiments were carried out on the basis of the developed program "DUST-2", which can be used to assess the microclimate in the passenger compartment, to improve the operation of the ventilation system, as well as to change and improve the design inside the cabin.

Refereces

1. **Rojas, J.C.; Sánchez, N.E.; Schneider, I.; Teixeira, E.C.; Silva, L.F.O.** 2019. Exposure to nanometric pollutants in primary schools: Environmental implications, Urban Clim. 27: 412-419.
2. **Zamberland, D.C.; Halmenschelager, P.T.; Silva, L.F.O.; Da Rocha, A.; Rocha J.B.T.** 2020. Copper decreases associative learning and memory in Drosophila melanogaster, Sci. Total Environ 710: 135306.
3. **Kumar, P.; Robins, A.; Vardoulakis, S.; Britter, R.** 2010. A review of the characteristics of nanoparticles in the urban atmosphere and the prospects for developing regulatory controls, Atmos. Environ. 44 (39): 5035-5052.
4. **Rizza, V.; Stabile, L.; Vistocco, D.; Russi, A.; Pardi, S.; Buonanno, G.** 2019. Effects of the exposure to ultrafine particles on heart rate in a healthy population, Sci. Total Environ. 650: 2403-2410.
5. **Pacheco-Torgal, F.; Diamanti, M.V.; Nazari, A.; Granqvist, C.G.; Pruna, A.; Amirkhanian S.** 2019. Nanotechnology in Eco-efficient Construction, Woodhead Publishing Series in Civil and Structural Engineering, Cambridge, 705-754.
6. **Guo, L.; Johnson, G.R.; Hofmann, W.; Wang, H.; Morawska, L.** 2020. Deposition of ambient ultrafine particles in the respiratory tract of children: A novel experimental method and its application, Journal of Aerosol Science 139: 105465.
7. **Gao, R.; Sang, N.** 2020. Quasi-ultrafine particles promote cell metastasis via HMGB1-mediated cancer cell adhesion, Environ. Pollut. 256: 113390.
8. **Chen, X.C.; Cao, J.J.; Ward, T.J. Tian, L.W.; Ning, Z.; Kumar, N.G.; Aquilina, N.J.; Lam, S.H.; Qu, Y. L.; Ho, K.F.** 2020. Characteristics and toxicological effects of commuter exposure to black carbon and metal components of fine particles (PM2.5) in Hong Kong. Sci, Total Environ742: 140501.
9. **Hudda, N.; Kostenidou, E.; Sioutas, C.; Delfino, R.J.; Fruin, S.A.** 2011. Vehicle and driving characteristics that influence in-cabin particle number concentrations, Environmental Science and Technology 45(20): 8691-8697.
10. **Bin, Xu; Xiaokai, Chen; Jianyin, Xion**. 2016. Air quality inside motor vehicles' cabins: A review, Indoor and Built Environment 27(4): 452-465.
11. **Ljung, S.** 2019. CFD simulation of particle matter inside an automotive car and the purification efficiency of cabin air purifier. Appendix B. Particle Fate, 58 p.
12. **Samarsky, A.A.; Mikhailov, A.P.** 2001. Mathematical Modeling. Moscow: Fizmatlit, 320 p.
13. **Zgurovsky, M.Z.; Skopetsky, V.V.; Khrushch, V.K.; Biliaiv, M.M.** 1997. Numerical modeling of the spread of pollution in the environment. Kiev: Naukova dumka, 368 p.